

## A novel fluorophore for two-photon-excited single-molecule fluorescence

P.J. Schuck<sup>a</sup>, K.A. Willets<sup>a</sup>, D.P. Fromm<sup>a</sup>, R.J. Twieg<sup>b</sup>, W.E. Moerner<sup>a,\*</sup>

<sup>a</sup> Department of Chemistry, Stanford University, Stanford, CA 94305, United States

<sup>b</sup> Department of Chemistry, Kent State University, Kent, OH 44242, United States

Received 28 December 2004; accepted 14 March 2005

Available online 13 April 2005

### Abstract

We have studied the two-photon excited fluorescence properties of a new fluorophore, DCDHF-6, at single-molecule and bulk concentrations. This molecule features several beneficial properties including suppressed blinking, high fluorescence quantum yield, and viscosity-dependent fluorescence. Here, analysis of the two-photon excited fluorescence (TPF) behavior of single DCDHF-6 molecules demonstrates their applicability to experiments combining single-molecule and two-photon microscopy. A method is developed for measuring the absolute two-photon absorption cross-section  $\delta$  of a single dye copy, and DCDHF-6 is shown to have a  $\delta$  of 44 GM at an excitation wavelength of 940 nm.

© 2005 Elsevier B.V. All rights reserved.

**Keywords:** Single-molecule fluorescence; Nonlinear optical chromophore; Two-photon fluorescence; Single-molecule spectroscopy

Two-photon excited fluorescence (TPF) microscopy is a well-known imaging method used widely in both the biological and physical science communities [1–3]. Due to the nonlinear dependence of two-photon absorption (TPA) on excitation intensity  $I$  ( $\text{TPA} \propto I^2$ ) and sample transparency at the excitation wavelength, TPF occurs only within the focal volume of the focused excitation beam where intensity is highest, allowing subsurface imaging without cleaving, damaging, or otherwise altering the sample, and without appreciable photobleaching of fluorophores adjacent to the focal volume. An ideal TPF dye would have as large a TPA cross-section  $\delta$  as possible; common dyes have  $\delta$ s in the order of  $10 \times 10^{-50} \text{ cm}^4/\text{s}/\text{photon} = 10 \text{ Goeppert-Mayer (GM)}$  [4] and are utilized almost exclusively in bulk concentrations so as to generate detectable amounts of fluorescence signal. Relatively few single-molecule TPF experiments exist in the literature [5–9], despite the fact

that such experiments could combine the subsurface imaging capabilities of TPF microscopy with the many advantages of single-molecule microscopy (working inside the ensemble average, nanometer-scale sensitivity, etc.) [10]. In order to combine TPF and single-molecule microscopy, however, a fluorophore with both a large  $\delta$  and excellent single-molecule fluorescence properties, e.g., high quantum yield and photostability, is required.

The search for such molecules has led us to consider a relatively new class of single-molecule fluorophores, the DCDHFs [11]. The DCDHF dyes, which contain an amine donor and a dicyanodihydrofuran (DCDHF) acceptor, were originally developed as nonlinear optical (NLO) chromophores for use in photorefractive polymers/glasses [12]. Though most other NLO chromophores are non- or weakly fluorescent, the DCDHFs are excellent single-molecule emitters, and their single-molecule imaging capabilities have been recently documented [11,13]. These molecules have strong one-photon absorption, high quantum yield, weak triplet-state bottlenecks, and high photostability. Various derivatives

\* Corresponding author.

E-mail address: [wmoerner@stanford.edu](mailto:wmoerner@stanford.edu) (W.E. Moerner).

have absorption and fluorescence across the visible spectrum [11], and the DCDHFs show emissive properties sensitive to local rigidity [13]. Modification of the DCDHF structure allows for the electronic and morphological properties to be tuned so that they may be tailored to many environments and applications. The DCDHFs also possess a moderate hyperpolarizability ( $\beta_0$ ), large polarization anisotropy ( $\delta\alpha_0$ ), and a significant ground state dipole moment ( $\mu_g$ ) – all potentially valuable properties that are absent in virtually all other single-molecule fluorophores. In this work, we report on the single-molecule TPF properties of DCDHF-6 (formal name 2-dicyanomethylene-3-cyano-5,5-dimethyl-4-(4'-dihexylaminophenyl)-2,5-dihydrofuran), which is a representative member of the DCDHF class of dyes, in this case with a dihexylamino donor group.

Single-molecule (bulk) concentration DCDHF-6 samples were spun onto a glass cover slip from a solution of  $\sim 10^{-10}$  ( $\sim 10^{-4}$ ) M dye in poly(methyl methacrylate) (PMMA)/toluene, 1% m/m. The structure of DCDHF-6 is shown in Fig. 1(a) and details of its synthesis are reported elsewhere [14]. TPF was measured with a confocal sample-scanning configuration [15]. A mode-locked Ti:sapphire laser with repetition rate of  $\sim 76$  MHz and 120 fs pulses was used for excitation through the epifluorescence port of an inverted optical microscope (Nikon TE300). Pump wavelengths  $\lambda_{\text{pump}}$  were tuned between 790 and 960 nm. The linearly polarized excitation beam was focused using a  $1.4N.A.$ ,  $100\times$  oil objective. TPF was collected by the same objective

and passed through three spectral filters, which effectively transmit emission with wavelengths between 460 and 700 nm while attenuating the laser light with an optical density (OD)  $> 18$ . A large aperture (200  $\mu\text{m}$ ) was used in the detection path to further reduce backgrounds from scattered excitation light. The fluorescence is either focused onto a single-photon counting avalanche photodiode (APD) for broadband collection or dispersed by a spectrometer onto a liquid-nitrogen-cooled Si charge-coupled device (CCD) camera (Roper Scientific) for spectral detection. For TPF time-dependent analysis, each photon detected by the APD is time stamped by a time-correlated single-photon counting (TPSPC) board (PicoQuant, TimeHarp 200) [16].

The detected TPF signal from a bulk dye concentration film, measured as function of average excitation power, is plotted in Fig. 1(b). The best-fit line through the data has a slope = 2 on a log–log scale, confirming that the detected fluorescence is quadratically dependent on incident excitation intensity and is the result of TPA. One-photon and two-photon fluorescence spectra from a bulk concentration film are shown in Fig. 1(c). Both spectra have the same peak wavelength ( $\lambda_{\text{peak}} = 525$  nm) and full width at half maximum (FWHM  $\approx 60$  nm), though the two-photon spectrum may exhibit a slight amount of broadening relative to the one-photon spectrum near  $\lambda_{\text{peak}}$  on the long wavelength side.

As demonstrated by the confocal scanning image in Fig. 1(d), we observe TPF from individual DCDHF-6 molecules in a PMMA film. Fig. 1(d) is a  $10\ \mu\text{m}$  by  $10\ \mu\text{m}$  (200 by 200 pixel) image acquired with an average incident power of  $260\ \mu\text{W}$  at  $\lambda_{\text{pump}} = 930$  nm and dwell time of 10 ms/pixel. Fig. 1(e) shows the area-integrated TPF intensity from a single molecule as a function of time. Each detected fluorescence photon in the time trace is time stamped [16], and time traces were collected for 130 individual DCDHF-6 molecules. Similar to one-photon fluorescence [11], blinking was not observed on a 100 ms time scale from  $>80\%$  of the molecules, demonstrating excellent stability.

The total number of detected TPF photons  $N_{\text{Tot}}^{\text{TPF}}$  per molecule was determined by integrating individual single-molecule time traces, yielding the histogram in Fig. 2(a). The characteristic  $N_{\text{Tot},0}^{\text{TPF}}$ , defined here as the  $e^{-1}$  value of a single exponential fit to the distribution, is  $6024 \pm 730$  for two-photon excitation. Because the distribution in Fig. 2(a) is exponential and not Gaussian, the process leading to the loss of fluorescence in these molecules is simple Poisson (i.e., single-step photobleaching) and not due to a thermal bleaching process [5].  $N_{\text{Tot},0}^{\text{TPF}}$  is much less than the mean number of detected photons of 250,000 for one-photon excitation [11]. Because relatively high excitation intensities are employed for single-molecule (versus bulk) TPF studies, this result is consistent with previous TPF studies where the photobleaching rate was shown to be strongly dependent on

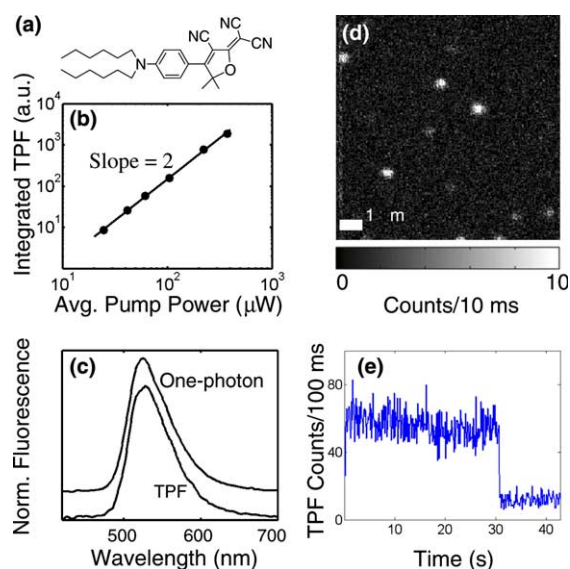


Fig. 1. (a) Structure of DCDHF-6. (b) A log–log plot demonstrating the quadratic dependence of TPF on average excitation power. (c) One- and two-photon fluorescence spectra from DCDHF-6, where the one-photon spectrum has been vertically offset for clarity. (d) TPF scanning image of single DCDHF-6 molecules in a PMMA film. (e) Area-integrated TPF intensity of a single molecule as a function of time, 100 ms averaging interval.

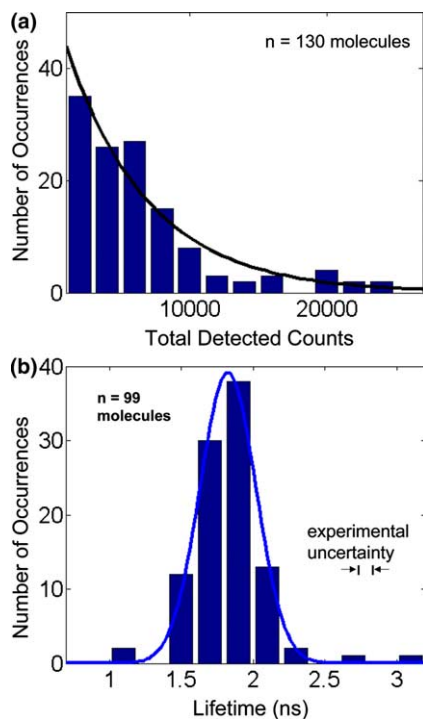


Fig. 2. (a) Histogram of total detected TPF photons from single-molecule time traces and an exponential fit to the distribution, yielding an  $e^{-1}$  value of  $6024 \pm 730$  photons. A histogram of single-molecule TPF lifetimes of DCDHF-6 in PMMA is shown in (b). The lifetime distribution is fit to a Gaussian; fit parameters are given in the text.

two-photon excitation power [17]. The increased photobleaching is attributed to higher-order photon interactions within the focal volume [8,17,18]. We note, however, that enough TPF photons are detected for both the imaging (see Fig. 1(d)) and lifetime determination (see Fig. 2(b)) of individual DCDHF-6 molecules. The total number of emitted photons is given by  $N_{\text{Tot}}^{\text{TPF}}$  divided by the collection efficiency  $\phi$  of our experimental set-up (measured to be 5.1%) and is, on average, equal to  $\sim 120,000$  per molecule before photobleaching.

The TPF time records of photon arrival times relative to the excitation pulse yield fluorescence lifetime information for individual molecules excited via two-photon absorption. The lifetime data from each molecule is deconvoluted from the instrument response function (IRF) and fit to a single exponential using maximum likelihood estimation. A histogram of lifetimes from 99 single molecules is shown in Fig. 2(b). All molecules were checked for digital photobleaching to ensure the collected emission was from a single molecule, and only lifetime data from molecules with more than 1000 detected photons are reported, ensuring adequate fitting accuracy. The statistically expected width of the histogram due to limited observation time is  $\sim 150$  ps [19], which is based on the minimum count number, the average excited state lifetime, and the time bin specifications

of our detector and related electronics. A Gaussian fit to the distribution has a standard deviation of 200 ps, somewhat larger than the expected statistical width, and is attributed to microscopic heterogeneity of the polymer film. The ensemble-averaged TPF lifetime of 1.8 ns is shorter than the average one-photon excitation lifetime of 2.5 ns [13], providing possible evidence that separate recombination pathways are accessed for two-versus one-photon excitation. Samples for the one- and two-photon single-molecule lifetime experiments were prepared similarly and consist of DCDHF-6 molecules distributed throughout a  $\sim 50$  nm thick PMMA film on coverglass. Embedding the molecules in the PMMA matrix is expected to reduce surface-molecule interactions and, therefore, surface effects on lifetime. We suspect the reduction in lifetime for TPF is due to an increase in non-radiative relaxation, which is most likely related to the large pump intensities present in the focal volume. Previous electronic structure calculations show that DCDHF molecules are susceptible to a twist of the dicyano group when excited, which leads to non-radiative relaxation [13]. It is possible that this twist is enhanced by either the resonant absorption of a third infrared photon or by a softening of the surrounding polymer matrix due to localized heating. Such a process leads to a reduction in the TPF quantum yield.

Usually, TPA cross-sections are determined via measurements on bulk-concentration samples such as those found in [4,20]. Here, we develop a new method based on single-molecule imaging where we use the detected TPF count rates from single emitters to determine the TPA cross-section. The TPF signal from a single molecule centered in the focused, diffraction-limited excitation spot is given by

$$\langle \text{TPF}(t) \rangle = \frac{1}{2} \cdot \phi \cdot \eta_2 \cdot \delta \cdot \frac{g_p}{f\tau} \cdot \frac{\pi^2 (N.A.)^4}{\lambda_{\text{pump}}^4} \cdot \langle P(t) \rangle^2, \quad (1)$$

where  $\langle \text{TPF}(t) \rangle$  = time-averaged TPF count rate,  $\phi$  = collection efficiency = 5.1%,  $\eta_2$  = TPF quantum yield,  $\delta$  = TPA cross-section,  $g_p = 0.588$  for  $\text{Sech}^2(t)$  pulse shape,  $f$  = repetition rate (76 MHz),  $\tau$  = pulse width (120 fs), and  $\langle P(t) \rangle$  = average incident excitation power. This method simplifies the TPA cross-section determination in two ways: (1) the dye concentration within the focal volume is now known exactly and is equal to 1, and (2) only knowledge of the peak intensity at the center of the excitation focus is needed; the full three-dimensional integral over the entire focal volume is no longer required. This is notable since the volume integral can be a significant source of error in the determination of the TPA cross-sections due to aberration in the imaging optics and nonlinear effects (self-focusing, etc.) in the focal volume related to the extremely high peak intensities present in TPA experiments. On the other hand, Eq. (1) presumes that the molecule has a transition moment

aligned with the electric field of the pumping light, an issue we now discuss.

The average TPF count rate was determined for each single-molecule time trace. The TPF count rate from a single DCDHF-6 molecule, however, is related to its orientation in the PMMA film relative to the excitation polarization. To compare the  $\delta$  values found using Eq. (1) to values of  $\delta$  in the literature determined from bulk solutions and films, which are averages over all possible molecular orientations, we correspondingly compute the ensemble average of all  $\langle \text{TPF}(t) \rangle$  values from the individual single-molecule time traces. This has the effect of extracting from the single-molecule measurements a value of  $\delta$  that will be most comparable to that from bulk studies. In a situation where the single-molecule orientations are well-defined or directly measured by polarization methods, the true peak value of  $\delta$  could be extracted. For our situation, the average of  $\langle \text{TPF}(t) \rangle$  was found to be 493 counts/s for an average excitation power of 260  $\mu\text{W}$  at  $\lambda_{\text{pump}} = 930$  nm. Inserting this into Eq. (1) along with the other known parameters yielded an orientationally-averaged  $\delta$  for DCDHF-6 of  $38 \pm 11$  GM at  $\lambda_{\text{pump}} = 930$  nm. In calculating  $\delta$ , we have made the common assumption [4] that  $\eta_2 =$  one-photon fluorescence quantum yield  $\eta_1$  in PMMA = 92% [11]. The validity of this assumption is based primarily on the similarity of the one- and two-photon fluorescence spectra in Fig. 1(c). However, the reduced TPF lifetime may indicate a reduction in  $\eta_2$  relative to  $\eta_1$  [21], in which case the values of  $\delta$  reported here must be adjusted accordingly.

To gain information about the TPA tensor of DCDHF-6, we performed bulk measurements of TPF for linear and circular excitation polarizations. We obtained a value of 1.45 for the ratio of TPF signals from linear versus circular polarization, confirming that the tensor is diagonal with one dominant element [9,22]. Because the tensor contains only one dominant element, TPA (and TPF if the absorption and emission dipoles are assumed collinear) has a  $\cos^4 \theta$  angular dependence for linearly polarized excitation, where  $\theta$  is the angle between the excitation polarization and the molecular transition dipole. For  $N.A. = 1.4$ , the collection efficiency of the microscope objective is equal for all molecular orientations and, therefore, contributes no angular dependence to the collected TPF signal distribution [23]. Unlike samples fabricated by spin coating dye solution directly onto the glass substrate, where molecules may orient preferentially towards the surface plane (due, for example, to electrostatic interactions with the surface) [9,24], the DCDHF-6 molecules are embedded in a polymer matrix and little, if any, preferential orientation is expected. Under these circumstances, the orientationally-averaged TPF will be 5 times smaller than when all molecules are aligned with the excitation polarization. Since the  $\theta$  dependence and polarization are

known, in principle the molecular orientation distribution can be determined from the distribution of single-molecule TPF signals. However, absolute calibration requires knowledge of the orientation of at least one molecule in the sample. This is not known for the sample discussed here, and since the interpretation of the single-molecule TPF signal distribution could be ambiguous, we therefore base our analysis on the ensemble-averaged TPF value from the single-molecule TPF time traces.

To confirm the accuracy of the single-molecule method for determining  $\delta$ , a bulk measurement was also performed. Following the approach described in [20], a value for  $\delta$  of  $33 \pm 10$  GM was found by comparing the one- and two-photon fluorescence from a bulk concentration film. Within experimental error, this value is nearly equal to the  $\delta$  derived above. It is expected that the single-molecule derivation of  $\delta$  would be slightly larger than the bulk value since molecules oriented nearly orthogonal to the incident polarization, which emit TPF signal below the noise floor of the detector and contribute extremely small effective TPA cross-sections to the overall average, are not detected in the single-molecule experiment and are therefore left out of the calculation.

A two-photon excitation (TPE) spectrum for DCDHF-6 in PMMA is shown in Fig. 3. The bulk sample was used to determine the relative wavelength dependence, but the absolute  $\delta$  calibration is from the 930 nm single-molecule measurement above. We find that DCDHF-6 has a maximum  $\delta = 44 \pm 13$  GM at  $\lambda_{\text{pump}} = 940$  nm. For comparison, the bulk one-photon absorption curve, plotted versus twice the one-photon absorption wavelength, is also presented in Fig. 3. The peak of the TPE spectrum is blue-shifted relative to

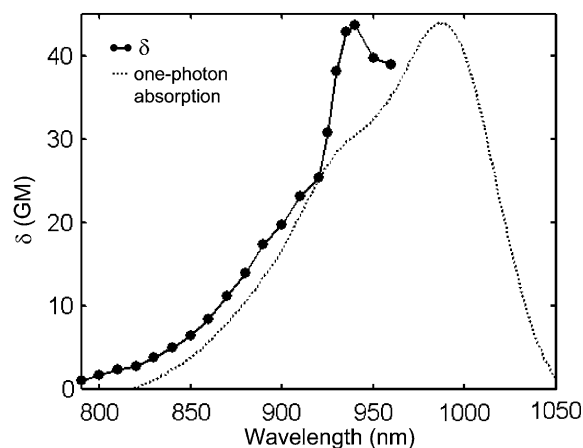


Fig. 3. The two-photon excitation spectrum (connected circles) and one-photon absorption spectrum (dotted line) for DCDHF-6 in PMMA. DCDHF-6 has a maximum  $\delta$  of 44 GM at  $\lambda_{\text{pump}} = 940$  nm. For comparison, the one-photon absorption spectrum is plotted versus twice the one-photon absorption wavelength.

Table 1  
Comparison of DCDHF-6 TPA cross-section with other dyes

Dye	Matrix/solvent	Wavelength (nm)	$\delta$ (GM)
DCDHF-6	PMMA	940	44
Rhodamine 6G <sup>a</sup>	Methanol	800	30
Fluorescein <sup>a</sup>	H <sub>2</sub> O	780	37
AF-50 <sup>b</sup>	Benzene	800	1940
AF-50 <sup>b</sup>	PMMA	760	658

<sup>a</sup> Ref. [25].

<sup>b</sup> Ref. [20].

twice the absorption maximum of 496 nm, consistent with the behavior of other TPF dyes [4]. The short wavelength shoulders on both curves are interpreted as vibrational structure. As seen in Table 1, the DCDHF-6 TPA cross-section compares favorably with those for other commonly used TPF dyes and is larger than the  $\delta$  peak of 30 GM at 800 nm for Rhodamine 6G and the  $\delta$  peak of 37 GM at 780 nm for fluorescein [25]. In addition, the DCDHF-6 TPA peak wavelength of 940 nm is longer than the peak TPA wavelengths of most other TPF dyes. This is useful for biological applications since the longer wavelength is less likely to pump other cellular emitters. Some dyes, such as AF-50, have been specifically tailored for TPF and have extremely large TPA cross-sections, e.g.,  $\delta = 1940$  GM for AF-50 in benzene [20]. However, these dyes have not been studied at the single-molecule level so their single-molecule fluorescence characteristics are unknown.

In conclusion, we have imaged single molecules of the novel fluorophore DCDHF-6 using two-photon fluorescence microscopy. TPF analysis from single DCDHF-6 molecules yielded a TPF lifetime of 1.8 ns and a mean (detected)  $N_{\text{Tot,O}}^{\text{TPF}}$  of  $6024 \pm 730$ . We have developed a single-molecule method for determining absolute TPA cross-sections, finding an orientationally-averaged  $\delta$  for DCDHF-6 of 44 GM at the peak wavelength of  $\lambda_{\text{pump}} = 940$  nm. These properties, combined with their

other unique characteristics, should make the DCDHF dyes useful probes for single-molecule TPF experiments in a wide range of environments and applications.

### Acknowledgement

This work was supported in part by the U.S. National Institutes of Health, Grant No. GM065331.

### References

- [1] W. Denk, J.H. Strickler, W.W. Webb, *Science* 248 (1990) 73.
- [2] P.J. Schuck et al., *Appl. Phys. Lett.* 81 (2002) 1984.
- [3] C.M. Niell, S.J. Smith, *Annu. Rev. Physiol.* 66 (2004) 771.
- [4] C. Xu, W.W. Webb, *J. Opt. Soc. Am. B* 13 (1996) 481.
- [5] G. Chirico et al., *Biophys. J.* 84 (2003) 588.
- [6] M.K. Lewis et al., *Opt. Lett.* 23 (1998) 1111.
- [7] J. Mertz, C. Xu, W.W. Webb, *Opt. Lett.* 20 (1995) 2532.
- [8] E.J. Sanchez et al., *J. Phys. Chem. A* 101 (1997) 7019.
- [9] M.A. Bopp et al., *Appl. Phys. Lett.* 73 (1998) 7.
- [10] W.E. Moerner, M. Orrit, *Science* 283 (1999) 1670.
- [11] K.A. Willets et al., *J. Am. Chem. Soc.* 125 (2003) 1174.
- [12] O. Ostroverkhova et al., *ChemPhysChem* 4 (2003) 732.
- [13] K.A. Willets, P.R. Callis, W.E. Moerner, *J. Phys. Chem. B* 108 (2004) 10465.
- [14] M. He et al., *Proc. SPIE* 4802 (2002) 9.
- [15] W.E. Moerner, D.P. Fromm, *Rev. Sci. Instrum.* 74 (2003) 3597.
- [16] K.A. Willets et al., *Proc. SPIE* 5222 (2003) 150.
- [17] G.H. Patterson, D.W. Piston, *Biophys. J.* 78 (2000) 2159.
- [18] M.A. van Dijk et al., *J. Phys. Chem. B* 108 (2004) 6479.
- [19] M. Maus et al., *Anal. Chem.* 73 (2001) 2078.
- [20] N. Mukherjee, A. Mukherjee, B.A. Reinhardt, *Appl. Phys. Lett.* 70 (1997) 1524.
- [21] J.R. Lakowicz, *Principles of Fluorescence Spectroscopy*, Kluwer Academic, New York, 1999.
- [22] P.R. Monson, W.M. McClain, *J. Chem. Phys.* 53 (1970) 29.
- [23] J. Enderlein, T. Ruckstuhl, S. Seeger, *Appl. Opt.* 38 (1999) 724.
- [24] M. Lieberherr, C. Fattinger, W. Lukosz, *Surf. Sci.* 189–190 (1987) 954.
- [25] M.A. Albota, C. Xu, W.W. Webb, *Appl. Opt.* 37 (1998) 7352.